JOINT EUROPEAN TORUS JET

JET-R(90)01

A.J. Bickley, D.J. Campbell, C.D. Challis, J.G. Cordey, S. Corti, W.G.F. Core, G. Cottrell, H.P.L. de Esch, L. de Kock, T. Hellsten, T.P. Hughes, J. Jacquinot, O.N. Jarvis, T.T.C. Jones, P. Lallia, F.B. Marcus, W. Obert, G. Sadler, P. Smeulders, D.F.H. Start, D. Stork, P.E. Stott, A. Tanga, E. Thompson, P. van Belle and M. von Hellermann

# Proposal for 160keV $^3$He Injection and Combined NBI/RF Heating

# Proposal for 160keV $^3$He Injection and Combined NBI/RF Heating

A.J. Bickley, D.J. Campbell, C.D. Challis, J.G. Cordey, S. Corti, W.G.F. Core, G. Cottrell, H.P.L. de Esch, L. de Kock, T. Hellsten, T.P. Hughes, J. Jacquinot, O.N. Jarvis, T.T.C. Jones, P. Lallia, F.B. Marcus, W. Obert, G. Sadler, P. Smeulders, D.F.H. Start, D. Stork, P.E. Stott, A. Tanga, E. Thompson, P. van Belle and M. von Hellermann

***JET Joint Undertaking, Culham Science Centre, OX14 3DB, Abingdon, UK***

**ABSTRACT**

The possibility of He Neutral Beam Injection, especially $^3$He at 150–160 keV, would extend the JET operating parameters and improve the physics interpretation from diagnostics. Extensive Fokker-Planck simulations have been made of NBI and combined NBI/RF heating, considering beam-plasma, beam-beam, and plasma-plasma fusion for D-$^3$He, D-D, and triton burnup. High-energy, monoenergetic He beams should allow access to ion temperatures of 25-50 keV, and D-$^3$He fusion power of several hundred kW. Pumping of $^3$He has been demonstrated in a full JET Neutral Beam box, and powers of 8-10 MW at 155 keV of neutral $^3$He are possible, although He metastable formation may enhance trapping at the plasma edge.

Since the neutron production is due only to thermal D-D reactions, and beam-plasma reactions are measurable from the D-$^3$He gamma ray branch, much clearer measurements are possible of the thermal ion distribution function. Charge-exchange with the He beam allows new possibilities for diagnostics with ex recombination spectroscopy, and active and passive ex particle detection.

Detailed experiments, diagnostic measurements, and physics are proposed:

– Standard operation with $^3$He NBI
– Fusion product and charge-exchange measurements of ion velocity distributions
– Hot-ion-hot-plasma experiments at reactor temperatures, 25–50 keV
– Synergistic effects of combined NBI/RF heating
– Simulation of alpha particle thermalization and particle diffusion
– Effects of velocity distributions on sawteeth, fishbones, and Alfven instabilities
– High ion temperature plasmas with reduced fusion neutron emission using H, $^3$He and $^4$He NBI

## CONTENTS

## 1. INTRODUCTION

Important results have previously been obtained on alpha particle simulations and D-$^3$He fusion in JET by ICRF [1,2,3]. With the availability of 8 PINI's in a JET NBI box in Octant 4 with energy 140-160 keV, and ultimately 8 PINI's on Octant 8, it is possible to consider injecting helium [4] and, in particular, 160 keV $^3$He into JET. These beams, especially if used in conjunction with ICRH, would allow a wide range of new experiments. The main goals of these experiments are summarized as:

- Measure D-$^3$He Fusion with NBI only
- Combine NBI and RF to look for synergistic effects
- Use NBI as a precise particle source for RF heating and alpha transport.
- Maximize ion heating.
- Study beam effects on instabilities.
- Verify diagnostic measurements (especially for fusion products and charge exchange) and code comparisons.
- Provide a means of reducing neutron generation during operation.

In this proposal, detailed Fokker-Planck calculations of fusions rates from 160 keV $^3$He injection are presented, without and with combined RF/NBI heating, along with a detailed discussion of physics, diagnostics, and technological aspects.

The general presentation is followed by specific proposals for experiments. These include:

1. Standard Operation with 160 keV $^3$He NBI

2. Fusion Product and Charge-Exchange Measurements of Ion Velocity Distributions with 160 keV $^3$He NBI

3. Hot-Ion-Hot-Plasma Experiments at Reactor Temperatures with 160 keV $^3$He NBI

4. Synergistic Effects of Combined 160 keV $^3$He NBI and Minority ICRF Heating

5. Simulation of α–Particle Thermalization and Particle Diffusion with 160 keV $^3$He NBI

6. Effects of Velocity Distributions on Sawteeth, Fishbones and Alfvén Instabilities with 160 keV $^3$He Injection.

7. High Ion Temperature Plasmas with Reduced or Zero Fusion Neutron Emission using H, $^3$He and $^4$He NBI

## 2. FOKKER-PLANCK SIMULATIONS OF 160 KEV $^3$He NBI AND COMBINED NBI/RF

For neutral beam injection of 160 keV $^3$He, the reaction rate and Q depend critically on the ion temperature T of the deuteron target plasma, since the cross section σ for D-$^3$He peaks at $0.67 \times 10^{-28}$ m$^2$ at a center of mass energy of 240 keV, and is only equal to $0.029 \times 10^{-28}$ m$^{-2}$ for 160 keV $^3$He on a deuteron at rest. In what follows, we discuss the reactivity and Q as a function of T for various different approaches and codes, calculating the beam-plasma reaction rate. We then consider possible beam-beam rates if deuterium injection is also turned on and, finally, a case where the thermal ions merge completely with the beam slowing down distribution. Combined NBI/RF cases are presented and synergistic effects are discussed.

### 2.1 Beam-Plasma Reactions

In a region with uniform plasma parameters, the Q ≡ (Fusion Power)/(Input Heating Power), for beam-plasma reactions, is given by

$$Q \equiv \left(\frac{Nd}{Ne}\right) \overline{\sigma v} \, (N_e \, t_{slow}) \, (E_{fus}/E_{beam})$$

where $\overline{\sigma v} \equiv$ slowing-down averaged reaction rate, which is a function of the ion temperature.

$t_{slow} \equiv$ slowing-down time of $^3$He on d-plasma

$N_d, N_e \equiv$ deuteron and electron density

$E_{fus} = 18353$ keV, $E_{beam} = 160$ keV $^3$He

With 160 keV $^3$He, the problem of calculating $N_e t_{slow}$ is simplified, since $^3$He slows down on ions over a wide range of plasma parameters. The critical energy for injection of a mass $A_{beam}$ into a plasma with A/Z = 2, such as deuterium or carbon, is $W_{crit} \approx (9\ T_e)\ A_{beam}$, independent of charge. For $^3$He (or T), $W_{crit}$ is 27Te, so that for Te ≥ 5.7 keV, the 160 keV $^3$He diffuses and thermalizes predominantly on ions. In this regime, $N_e\ t_{slow} \approx 3 \times 10^{18}$ m$^{-3}$ sec, and Q becomes proportional to σv. Zeff, the effective charge, has no effect on $t_{slow}$, but only affects the ratio $N_d/N_e$.

The results are shown in fig. 1 for several methods:
In the SNAP/SLOWDOWN code [5] the slowing down time and time-averaged $\overline{\sigma v}$ are found by integrating the $g_e$, $g_i$ functions from [6] and calculating the $\overline{\sigma v}$ at each velocity. The slowing down times are close to the simplified Stix formula [7]. The electron and ion temperatures are taken to be equal, but the result has been found to be almost independent of $T_e$ for $T_e$ > 5 keV. In Fig. 1, Q is plotted versus ion temperature, rising from Q = 0.125% at 5 keV to Q = 1.8% at 35 keV, following the approximate power law $T^{1.37}$. In this code, the lower integration limit for slowing down is 1.5 times the ion temperature.

These calculations were repeated using a simplified Fokker-Planck model [8], referred to as F-P. The tail causes slightly higher Q at 5 keV, and significantly larger Q at high energy, rising from Q = 0.155% to 1.55% for $T_i$ = 5 to 20 keV, a power law of $T^{1.66}$.

An improved Fokker-Planck formulation has been used [9] which includes electron and ion energy diffusion to calculate the beam distribution function and the fusion reaction rate, here referred to as HEBDPL (Helium Beam, D-Plasma). The results agree very closely with the other Fokker-Planck results at low $T_i$. However, as the temperature is increased to 35 keV, Q rises more slowly to 2.2%. The slowness of rise is due to the fact that the integration is extended down to 1.5 $V_{thermal}$, where $V_{thermal} \equiv (2T_i/m_i)^{1/2}$. At 160 keV $^3$He, and $T_i$ = 35 keV deuterium, the injection velocity is only 1.75 $V_{thermal}$, so the fast ion density and slowing down time fall, since fewer particles are considered to be fast ions.

However, this underestimates the true fusion rate, since the "thermal" $^3$He at high ion temperature will also have a large reactivity, from $^3$He plasma - D plasma reactions. We will consider this additional reactivity later.

In summary, all of the different calculation methods are fully consistent and give very similar results at low temperatures.

## 2.2 Beam-Beam, Plasma-Plasma, and Hot-Ion-Hot-Plasma Mode

For this discussion, it is important to understand where beam-beam and plasma-plasma reactions are separate and distinct- and where they merge and become indistinguishable. The access to the two regimes depends on the fuelling, pumping, and energy confinement properties of the plasma. We consider injection of 160 keV, $^3$He, and 80 or 140 keV D.

A key dividing parameter is the lower velocity limit for integrating the slowing down distribution of injected fast ions, which is 1.5 $V_{th}$. For deuterium at $T_i$ = 35.5 keV$_{th}$, 1.5 $V_{th}$ corresponds to beam energies of 80 keVdeuterons and 120 keV $^3$He. Ions slowing down below 1.5$V_{th}$ are considered part of the thermal ion distribution. In present JET discharges, with ion temperatures of 25 keV and averaged injection energies of 60-75 keV, we are already in the regime where beam-beam and plasma-plasma are starting to merge. In some JET shots, the calculated fast ion density on axis equals or exceeds the spectroscopically measured deuteron density, and the entire axial neutron emission can be explained as beam-beam only [10].

To reach the regime where beam ions become a large fraction of the deuteron density, the fuelling must be dominated by the fast ions. The electrons must have good energy confinement to be able to heat up so the critical energy, $9A_oT_e$, exceeds the beam energy and fast ions thermalize primarily on other ions. In JET, where $T_e \approx T_i$ /3 in the hot ion H-mode, this condition is satisfied with $T_e$ = 8 keV, giving $W_{crit}$ = 144 keV for deuterons. Let us consider the maximum ion temperature that may be obtained with 160 keV $^3$He injection, with or without additional 80keV or 140 keV deuteron injection. If we assume that all $^3$He and D ions are provided by the beams, then without any energy loss and ignoring ohmic heating at high Te, and radiation losses:

$$N_{He} E_{He} + N_D E_D = 1.5 [N_{He} T_{He} + N_D T_D + N_e T_e + N_I T_I]$$

where N is the total number, and I denotes impurity ions.

With the simplifying assumptions and definitions:

$$N_I = 0, T_i \equiv T_{He} = T_D = T_I, T_e = T_i/3,$$
$$N_e = 2N_{He} + N_D, \alpha \equiv N_D/N_{He}, E_{He} \equiv 160 \text{ keV}$$

then we obtain:

$$T_i = \frac{160 + \alpha E_d}{2.5 + 2\alpha}$$

The results are listed in Table I for the cases: $\alpha$ = 0 (pure He), 1 (equal), 2 (equal electron contribution), $\infty$ (pure D);$E_d$ = 0 (cold D), 60 (80 keV beam av), 80 (140 keV beam av), 140 (max). Note that a mixed deuterium beam extracted at 140 keV only has an 80 keV average, due to poor neutralization of the high energy component.

**Table I - Maximum Ion Temperature (keV)**

| $\alpha$ / $E_d$ | 0 | 1 | 2 | 5 | 10 | $\infty$ |
|---|---|---|---|---|---|---|
| 0 | 64 | 36 | 25 | 13 | 7 | 0 |
| 60 | 64 | 49 | 43 | 37 | 34 | 30 |
| 80 | 64 | 53 | 49 | 45 | 43 | 40 |
| 140 | 64 | 67 | 68 | 69 | 69 | 70 |

For example, with $E_D$ = 60 and $\alpha = \infty$, the 30 keV maximum for no energy loss and no impurities may be compared with the $T_i$ = 25 keV measured in a JET experiment with impurities present. Note that the 25 keV is the measured impurity ion temperature. At these high temperatures, with significant mixing of the beam and thermal component, the impurity-background thermalization needs to be carefully considered.

With $E_D$ = 0, the maximum ion temperature decreases from a maximum of 64 keV to below 10 keV for large amounts of cold deuteron fuelling.

## 2.3 Example of Hot-Ion-Hot-Plasma Mode

In a case which we will consider in some detail, take $E_{He}$=160 keV, $E_D$ = 80 keV, $\alpha$ = 2, giving $T_i \approx 50$ keV, and $T_e$ = 16 keV, and further assume that $n_e = 4 \times 10^{19}$

$m^{-3}$, $n_D = 2 \times 10^{19}$ $m^{-3}$, $n_{He} = 1 \times 10^{19}$ $m^{-3}$. The results are shown in Table II. For $T_i$ = 50 keV deuterons, 1.5 $V_{th}$ corresponds to cut-off energies of 169 keV $^3$He and 113 kV D, both values above the actual injection energy. The critical energy for $T_e$ = 16 keV is 432 keV for $^3$He and 288 keV for deuterium.

In this regime, where injected ions do not slow down on other ions because of their velocity, the dominant mechanisms are ion pitch angle scattering, some ion-ion thermalization, and a slow ion-electron transfer. From the single particle point of view, the slowing down times of 80 keV D and 160 keV $^3$He on electrons only, at 16 keV, are 1.77 sec and 0.67 sec, which we shall later assume to be the particle replacement time required. From an ion distribution point of view, the electron - $^3$He ion equipartition time is 1.04 sec. The self-collision time of deuterons is 0.33 sec and of He is 0.05 sec, so the ions will be completely pitch-angle scattered.

The axial pressure of such a plasma gives 7.3% toroidal beta on axis at 3.45 T, consistent with 2.5 times the average beta at the Troyon limit of a 4 MA plasma. The energy confinement time of a 4 MA H-mode plasma can be about 1 sec, making all characteristic loss times to be of order 1 sec.

The reactivity of the plasma can be estimated in two ways. If it is assumed that the injected $^3$He and deuterium have self-scattered to become isotropic Maxwellian distributions with $T_i$ = 50 keV, then $\overline{\sigma v}$ becomes $0.56 \times 10^{-22} m^3/sec$, and with $E_{fus}$ = 18.353 MeV per fusion, the fusion power, which is 100% in charged particles, becomes 33 $kW/m^3$ on axis.

Another method is to assume that the injected particles pitch angle scatter, but do not thermalize into a Maxwellian distribution. This method probably overestimates the reaction rate, although particles could be both upscattered or downscattered in energy. The $\overline{\sigma v}$ from isotropic collision of 80 kV D with 160 kV $^3$He is $\overline{\sigma v} = 1.1 \times 10^{-22}$ $m^3/sec$, only double that of the 50 keV Maxwellians, giving 66 $kW/m^3$. If the axial power was extended over 15 $m^3$ of plasma, i.e. out to r/a = 0.4, then the fusion power output would be in the range of 500-1000 kw. In practice, the power will be less, but probably in the 100's of kW range. For this plasma, the postulated $N_e(0)$ T (0) $\tau_E$ is $2 \times 10^{21}$ $m^{-3}$keV sec, about double the record shot #20981, with similar parameters except for doubled temperatures due to a doubled injection energy. The fast proton density may build up to large values if the discharge time can be extended.

The required injected power to sustain this plasma is difficult to estimate, without knowing global profiles, etc. One method is to set the energy and particle replacement time of each species to the slowing down time on electrons, arguing that fast ions escape when they are thermalized. This gives the injected powers of Table II, leading to central Q values of 6-12%. The global powers just depend on the beam deposition profile. Note that with the injection power used here, similar profile shapes to #20981 would imply a global energy confinement time of 2 sec due to the doubled temperatures, at only 9 MW of total D and $^3$He input powers. Therefore, injection power totals closer to 10 MW $^3$He and 5 MW D will probably be required.

## TABLE II

## Proposed Operating Parameters for Hot-Ion-Hot-Plasma, Combined 160 keV $^3$He, 80 keV D Injection

| | |
|---|---|
| Helium 3 Injection Energy | 160 keV |
| Deuteron Injection Energy | 80 keV |
| $T_i$ | 50 keV |
| $T_e$ | 16 keV |
| $N_{eo}$ | $4\times10^{19}m^{-3}$ |
| $N_D = N_D$ (fast) | $2\times10^{19}m^{-3}$ |
| $N_{He} = N_{He}$ (fast) | $1\times10^{19}m^{-3}$ |
| Deutron Energy corresponding to 1.5 $V_{th}$ | 113 keV |
| Helium-3 Energy corresponding to 1.5 $V_{th}$ | 169 keV |
| Deuteron Critical Energy | 288 keV |
| Helium-3 Critical Energy | 432 keV |
| Slowing down time, D on electrons only | 1.77 Sec |
| Slowing down time, He on electrons only | 0.67 Sec |
| Electron - He Ion equipartition time | 1.04 Sec |
| Deuteron Self Collision Time | 0.33 Sec |
| He self-collision Time | 0.05 Sec |
| Axial Pressure | $3.42\times10^5$ Pa |
| Axial toroidal beta at 3.45T | 7.3% |
| Plasma Current to give av. beta = 0.4 peak | 4 MA |
| Energy Confinement, 4 MA H-mode | 1 Sec |
| $\overline{\sigma v}_{pp}$ plasma-plasma D - $^3$He, $T_i$ = 50 keV | $0.56\times10^{-22}m^3$/Sec |
| $\overline{\sigma v}_{bb}$ [mono-energetic, angle-averaged isotropic collisions of 80 keV D and 160 keV $^3$He] | $1.1\times10^{-22}m^3$/Sec |
| $E_{fus}$ (D - $^3$He) | 18.353 MeV |
| $P_{p\text{-}p} \equiv N_D N_{He} \overline{\sigma v}_{pp} E_{fus}$ | 33 kW/m$^3$ |
| $P_{b\text{-}b} \equiv N_D N_{He} \overline{\sigma v}_{bb} E_{fus}$ | 66 kW/m$^3$ |
| Assumed particle Deuteron replacement | 1.77 Sec |
| Assumed particle Helium-3 replacement | 0.67 Sec |
| Axial Deuteron power required | 144 kW/m$^3$ |
| Axial Helium-3 power required | 382 kW/m$^3$ |
| Global Deuteron power for axial power | 2.5 MW |
| Global Helium power for axial power | 6 MW |
| Range of axial $Q_{D\text{-}^3He}$ values | 6 - 12% |
| Total fusion power with 15m$^3$ uniform volume | 0.5-1.0 MW |
| Axial d-d neutron production | $2.47\times10^{15}$N/m$^3$.Sec |
| Projected $N_e(0)T_i(0)\tau_E$ | $2\times10^{21}m^{-3}$keV sec |

## 2.4 D-D Fusion Rates and Triton Burn-up

Although one of the aims of $^3$He injection is to minimize neutron production, temperatures of 50 keV can lead to a significant D-D reaction rate. With a deuteron density of $2 \times 10^{19} m^{-3}$, a neutron production rate (and an equal triton rate) of $2.47 \times 10^{15}$ neutrons/$m^3$·sec results. For a 15 $m^3$ volume, the total becomes $3.7 \times 10^{16}$ neutrons/sec, equal to the present highest neutron yield rate. This rate is proportional to the square of the deuteron density, whereas the D-$^3$He rate is proportional to the density. Therefore, relative rate adjustments are possible for minimizing neutron production.

In present JET discharges, the D-D reactions produce tritons, which slow down classically to the peak of the D-T cross section, and produce 14 MeV neutrons in this beam plasma process. In discharges analyzed so far, the thermalized tritons contribute relatively few fusions. However, in sustained 25-50 keV plasmas, the thermalized triton burnup may become comparable to the beam-plasma burnup, as is shown in Table III.

For tritons born at 1.011 MeV, the burnup fraction of a few percent is relatively independent of plasma conditions, for classical slowing down. At $T_i$ = 5 keV, assuming a particle confinement time of thermalized tritons of 1 sec, the thermal burnup probability is negligible. However, for 25 and 50 keV, the triton burnup in the thermal reactions also reaches a few percent. If the flat-top discharge time for triton production and particle containment times were longer than 1 sec, the burnup fraction would increase proportionally. Presently, only small volumes of $T_i > 25$ keV are obtained, and for only a short time. However, a peak of 50 keV gives a large volume with $T_i > 25$ keV, and the thermal burnup effect should become important.

## Table III Triton Burnup

$N_e = 4 \times 10^{19} m^{-3}$, $N_d = 2 \times 10^{19}$, $N_{He} = 1 \times 10^{19}$, $Z_{eff} = 1.5$

A. Beam-Plasma (Triton Born at 1.011 MeV)

| | | | |
|---|---|---|---|
| $T_e$ (keV) | 5 | 8 | 16 |
| $T_i$ (keV) | 5 | 25 | 50 |
| Slowing-down Time $t_s$ (sec) SNAP/SLOWDOWN | 0.90 | 1.35 | 2.19 |
| Averaged reaction rate $\overline{\sigma v}$ ($m^3$ $sec^{-1}$) | $7.8 \times 10^{-22}$ | $7.4 \times 10^{-22}$ | $6.6 \times 10^{-22}$ |
| Burnup Probability $N_d \overline{\sigma v}\, t_s$ | 1.4% | 2.0% | 2.9% |

B. Plasma-Plasma (Assume T Particle confinement $t_p = 1$ sec)

| | | | |
|---|---|---|---|
| $T_i$ (keV) | 5 | 25 | 50 |
| Thermal Plasma Reaction Rate $\overline{\sigma v}$ ($m^3$ $sec^{-1}$) | $1.3 \times 10^{-23}$ | $5.6 \times 10^{-22}$ | $8.7 \times 10^{-22}$ |
| Burnup Probability at $t_p = 1$ sec $N_d\, \overline{\sigma v}\, t_p$ | 0.026% | 1.1% | 1.7% |

### 2.5 Scaling of Beam-Beam and Plasma-Plasma Reaction Rates

Following the arguments of the previous sections, we can estimate the plasma ion temperature and the regime of operation. The relative role of beam-beam and plasma-plasma rates depends on the fast ion fraction, up to 100%, where they become similar. This is seen from the scalings in Fig. 2. The plasma-plasma reaction rate is plotted from 15 to 100 keV for a Maxwellian D-$^3$He plasma. The reaction rate increases by two orders of magnitude up to $1.55 \times 10^{-22}$ $m^3$ $sec^{-1}$.

The beam-beam reaction rates are calculated in the range where the 1.5 $V_{th}$ cut off remains valid, for 80 keV D and 160 kV $^3$He. The reaction rate varies by a factor of 2 going from $T_i$ = 5 to 20 keV, due to tail formation from beam energy upscattering. The reaction rate is similar to that of a Maxwellian plasma with $T_i$ = 50 keV. Also plotted is the monoenergetic 80-160 case, which has an equivalent energy to $T_i$ = 80 keV. Also shown are the corresponding 140 - 160 keV cases. The main point of these curves is that as the hot-ion-hot-plasma

regime is approached, several methods of calculation and assumptions on distribution functions give rates in the range 0.5 - 1.5 x $10^{-22}$ $m^3$ $sec^{-1}$. All that matters is the total product $N_D N_{He^3}$, and not whether particles are counted as beam or plasma. Depending on heating power assumptions, Q values on axis in the range of several percent, perhaps up to 10%, can be obtained, as in the example.

## 2.6 Profile Effects of NBI and Combined NBI/RF Heating

The combined NBI/RF Fokker-Planck code PION [11] is used with full profiles for beam deposition and self-consistent RF power deposition and velocity-distribution calculations. The PION code was tested against a full 2-D Fokker-Planck code. The D-$^3$He fusion reactivity is calculated for both beam-only and combined NBI/RF heating. The bulk plasma is deuterium, with assumed density and ion and electron temperature profiles. The code assumes the bulk plasma to be Maxwellian, and has one beam/minority species, $^3$He, whose distribution function self-consistently includes $^3$He beam injection and ICRH heating resonant with $^3$He. The effects of additional injection of a D-beam are included by assuming an appropriately higher D-plasma Maxwellian ion temperature. In these examples, Tion on axis equals either 25 keV or 50 keV, assumed to correspond to cases with cold deuterium fuelling or high power deuterium NBI, respectively. The ion and electron temperatures are taken to be a parabola squared, with the electron temperature 1/3 of the ion temperature. The electron density is taken to be 4 x $10^{19}m^{-3}$ on axis, with a parabola to the 0.55 power as a profile. No impurities are present, and ratios of $^3$He to D of 20% and 50% are considered, allowing for medium or long pulse build-up of $^3$He. A 20% ratio gives 0.58 x $10^{19}m^{-3}$ of $^3$He on axis. The peak deposition rates in $10^{19}m^{-3}s^{-1}$ for 8 MW are about: 2.0 on axis; 0.7 averaged inside r/a =0.5; and 0.3 averaged over the whole plasma. Without pumping or additional puffing, 20% or 50% minority correspond very roughly to 1 second and 3 seconds of injection, respectively, at this density. The beams are taken to be 10 MW of 160 keV $^3$He, and the ICRF is a dipole operating at the fundamental $^3$He frequency, with a $K_{11}$ peak of 5 $m^{-1}$.

For central ion and electron temperatures of 25 keV, the power deposition profiles for 20 MW of ICRF and 10 MW of NBI are shown separately in Fig. 3. The NBI profile was taken from separate beam deposition calculations (to be discussed). The RF deposition is self-consistently calculated by PION. The

deposition profiles are relatively independent of plasma temperature and minority fraction in the cases investigated. However, the average temperature and hence the reactivity depends on minority fraction. For the example chosen of 20% minority $^3$He, the average temperature of the $^3$He versus radius is shown in Fig. 4. The average temperature here is defined as the $^3$He distribution energy divided by 1.5 times the density, and is below 1 MeV.

The D-$^3$He fusion power calculated for several cases is shown in Fig. 5. The two curves are calculated with axial ion temperatures assumed to be 25 and 50 keV, both with 20% minority. For comparison, two points with Tion = 50 keV are shown, one with 50% minority, one with a parabolic temperature profile. The fusion rates are significantly higher at 50 keV than at 25 keV due to the increase in hot rarget reactivity. It is difficult to calculate Q values, since the amount of deuterium NBI power needed to help reach these temperatures is not known. If the deuterium NBI power is ignored, then with 10 MW of $^3$He NBI and Tion = 50 keV, the global Q values for D-$^3$He fusion are 4.3%, 3.2%, and 2.5% for RF powers of 0, 10 and 20 MW respectively. Similarly ignoring deuterium NBI power, the axial Q values in the absence of RF power are 1.2% at 25 keV and 5.3% at 50 keV. These values are consistent with previous local calculations of Q shown in Fig. 1.

In the most optimistic case with parabolic temperatures, 1 MW is produced. However, over a wide range of conditions several 100's of KW may be expected. It is also notable that with the chosen electron density and parabolic ion temperature profiles, a plasma with a peak ion temperature of 40 keV and central deuterium and tritium densities of $2 \times 10^{19} m^{-3}$ each would produce $10^{19}$ reactions/sec and 30 MW of D-T power in a 100 $m^3$ plasma, giving thermonuclear $Q_{DT}$ values of order 1. For the case of a deuteron density of $2.85 \times 10^{19}/m^3$ and 40 keV, the d-d thermonuclear rate becomes $10^{17}$ neutrons per second, a total d-d fusion rate of $2 \times 10^{17}$ reactions/sec, and a d-d fusion power above 100 kW.

Detailed fusion rate profiles of the data plotted in Fig. 5 are shown in Figs. 6 and 7. In Fig. 6 for 20% minority and Tion = 25 keV, the profiles with and without 20 MW of RF are shown. Both cases have 10 MW of $^3$He NBI. The RF significantly increases the fusion rate on axis and in the central plasma region. In contrast in Fig. 7, with $T_i$ = 50 keV, the fusion power increase is more moderate and slightly off-axis. This is because the reactivity is nearer to the maximum over much of

the plasma, and the RF improvement is smaller, and very small on axis. In this case, off-axis heating might be beneficial.

In Fig. 8, a comparison between 20% and 50% minority concentrations is made at 50 keV. Globally, the rate of the 50% minority is 89% of the 20% minority. the fusion rates are nearly equal everywhere, showing the reduced importance of minority fraction at high temperature.

In conclusion, a wide range of operating parameters are accessible. With $^3$He injection and high ion temperatures, RF coupling is efficient up to 50% minority concentrations. the synergistic effects of $^3$He beams and RF are most notable at lower ion temperatures. The key uncertainty remains the actual ion temperatures which can be achieved in JET experiments.

## 3. DIAGNOSTICS AND BEAM TECHNOLOGY

### 3.1 Gamma Ray Diagnostics

An extensive discussion of gamma diagnostics in JET for D-$^3$He plasmas has been presented [12]. A comfortable detection level of 16 MeV $\gamma$ rays is about $10^{16}$ D-$^3$He fusions per second, or about 30 kW, which is available from the experiments previously proposed. About 1 in 30000 reactions produces a $\gamma$-ray. Possible levels of several hundred kW of power, compared to the previous level of 100 kW, should provide more diagnostic opportunities for time-resolved behaviour and profile measurements. Also, since the rate is influenced by a high energy tail on the $^3$He beam due to energy diffusion on hot thermal ions, a sensitive study of this diffusion should be possible. In addition, the 100's of kW of protons generated isotropically provide opportunities for both p-Be and fast ion studies.

### 3.2 Neutron Diagnostics

The use of $^3$He injection into D plasmas allows a much cleaner use of neutron diagnosis than with D beams in D plasmas. There are no longer beam-beam or beam-plasma reactions mixed into 2.4 MeV neutron generation. Comparisons between calculated neutron emission from other ion temperature measurements and temperatures measured from neutron spectrometers should be much more accurate. Effects such as distortion of a Maxwellian ion temperature by beam ions can be studied. With radial measurements of neutron emission by the profile

monitor, a fully self-consistent comparison should be possible with profile measurements of ion temperature from charge-exchange spectroscopy.

Sawtooth studies with the profile monitor can be extended, since high ion temperatures giving high neutron yields can be measured, and the sawteeth in neutron signals will be due to the redistribution of thermal plasma only, although thermalization and heating from redistributed fast ions will complicate the analysis if data analysis intervals are too long.

### 3.3 Triton Burnup Measurements

If both D and $^3$He beams are used, high ion temperatures in the 25-50 keV range may be obtained, in which high D-D fusion and triton production rates may occur. The flux of triton slowing-down induced 14 MeV neutrons will be enhanced by burnup of thermalized tritons at high ion temperature. The 14 MeV signal on the silicon diode should then give information on both triton slowdown and the particle confinement time of thermalized tritons.

### 3.4 Charge-Exchange Spectroscopy

A detailed memo on the advantages on using charge-exchange spectroscopy with a 160 keV $^3He^0$ beam has been prepared [13]. An initial difficulty is that the diagnostic looks at octant 8, but the 140-160 kV beams are on octant 4. However, 140-160 kV PINIs will ultimately be installed on octant 8 at 140-160 keV.

Therefore, using this diagnostic immediately relies on adding one or several channels to octant 4. Using hydrogen or $^3$He injection at 80 keV on octant 8 is an option. The use of deuterium beams should be avoided for experiments where beam-beam and beam-plasma generation of D-D neutrons is not desired.

In addition to the thermal and beam ion velocity distribution functions and density, it should be possible to measure the beam density, $Z_{eff}$ and the motional Stark effect.

The advantages of $^3$He are a monoenergetic beam and a high (160 keV/3) ratio of energy to atomic mass number. This allows a very wide range of experiments. Recent experiments with Be have experienced problems with overlap of Be and He lines. It is thought that these problems can be overcome.

### 3.5 Passive Charge Exchange

The passive charge exchange system is being upgraded to study fast ions with up to 500 kV energy and mass selection. This will make it a useful tool for studying upscattering of injected $^3$He (relying on double resonant charge exchange) and high ion temperature plasmas.

### 3.6 Active Charge Exchange

A proposal has been made to use $^3$He diagnostic beams for an alpha particle diagnostic [14]. For D-T plasmas in JET, alpha particle velocity distributions up to 1.5 MeV could be measured by a charge exchange analyser looking at the beam, using $He^{++}$-$He^0$ double charge exchange.

With the beam currents of multi-MW $^3$He injection, high $^3$He minority concentrations, and reduced radiation levels compared to D-T operation, the measurement should allow a high signal/noise ratio. The diagnostic could study in detail the beam slowing down distribution, or the combined NBI/RF distribution with energies up to 2 MeV, which are characteristic of minority concentrations of 10% or greater.

### 3.7 Beam Technology

We have shown that 160 kV $^3$He beams have important advantages for high ion temperatures and physics and diagnostic studies. However, full power injection needs to be demonstrated. The JET testbed and octant 4 neutral beam box have demonstrated that 10 second pulses of $^3$He can be pumped using Argon frost. Due to perveance limits on the source and duct loading limits, a likely capability seems to be 8 MW per box of 8 PINI's of 155 keV neutral $^3$He into JET.

The cost of $^3$He is £150/bar.liter. An 8 PINI pulse of 10 MW injected for 2 sec is estimated to cost £60. This does not seem excessive.

Operation with 160 keV $^3$He is identical to 160 kV T injection from the point of view of bending magnets and beam optics. With present beam duct protection, considerations of stray fields determine the minimum plasma current. Operation is considered: safe with minimum currents of 4 MA in DN-XP and 5 MA in LIM; marginal with 3 MA in DN-XP and 4 MA in LIM; and unsafe with

3 MA in LIM and 3 MA and 4 MA in SN-XP. When new ducts are available co-injection will be safe for all currents above 2MA.

### 3.8 Beam Particle and Power Source

The maximum power available for $^3$He injection is estimated to be 8-10 MW from octant 4 at 155 kV, and 8-10 MW from octant 8 at 80 kV, both beams completely mono-energetic. With 8 MW at 155 keV, the axial particle source rate for central electron densities between 3 and 8 x $10^{19}$ $m^{-3}$ is 2 x $10^{19}$ He/$m^3$.sec. About 30-40% of the deposition is inside r = 0.5 meters, and an average deposition rate in this volume is 0.7 x $10^{19}$ He/$m^3$ sec. For the full 100 $m^3$, it is 0.3 x $10^{19}$ He/$m^3$ sec on average. In short pulse mode, the beam provides a precise source of He on axis, either for particle diffusion or RF heating studies.

### 3.9 Reduced Neutron Generation

Large neutron rates of several $10^{16}$/sec have been generated in JET which leads to a problem of induced vessel activation, limiting operation. With one or both beam boxes at 140-160 keV, the use of deuterium beams causes high neutron yields. Hydrogen beams are not acceptable at this energy due to low neutralization efficiency. $^3$He beams allow full use of the heating capability of NBI, while minimizing d-d neutron production, except in the hot-ion-hot-plasma mode of operation.

To minimize d-d neutrons under high ion temperature conditions, a suitable ratio of deuterium to hydrogen in the plasma can be chosen.

### 3.10 Injection of $^4$He, H and 80 keV $^3$He beams

The advantage of D-$^3$He operation is that gammas produced by the fusion reaction can be diagnosed, and $^3$He beams have excellent penetration into the plasma. However, there are also many experiments and advantages with $^4$He or H injection, which we now examine.

In Figs. 9, 10 and 11 the beam power deposition profiles per PINI with 8 PINI's per beam box, are plotted versus radius for 3 flat density profiles: 5 x $10^{19}$ $m^{-3}$, 1 x $10^{20}$ $m^{-3}$, and 2 x $10^{20}$ $m^{-3}$. The shinethrough is less than 10% for all cases shown.

The 8 curves are for each of the 4 gases, H, D, $^3$He, $^4$He at two energies, limited by either extraction voltage, extraction current, or bending magnet limits. The extraction energy (keV), species, and injected neutral power (MW) per PINI are: 80 H - 0.82; 80 D - 1.29; 80 $^3$He = 0.96; 80 $^4$He - 0.90; 110 H - 0.42; 140 D - 0.95; 160 $^3$He - 1.11; 120 $^4$He - 0.58. From Fig. 9, we see that 160 keV $^3$He has the second highest total power per PINI, 86% of 80 keV D. From Figs. 10 and 11 we see that it gives the best penetration at all densities, making it suitable for heating the highest density plasmas in JET.

At low densities, shinethrough can become a problem. For $Z_{eff} = 1$, with a density profile of a parabola to the 0.55 power, and 155 keV $^3$He injection, central electron densities of 1, 3 and $5 \times 10^{19} m^{-3}$ lead to shinethrough fractions of 63%, 25%, and 10% respectively. However, at low densities, the relative fraction of $^3$He ions in the plasma will lead to enhanced beam trapping. This effect also needs to be calculated at high density for high minority $^3$He fractions. Also, $Z_{eff}$ is greater than 1 at low density.

$^4$He injection has already been tested on the beam test stand, and can be pumped with Argon frost. The most interesting aspect of $^4$He injection is that it is an extremely efficient ion heater. The figure of merit for ion heating is the ratio $W_{crit}/E_{beam}$. This ratio is 16/9 times higher for A = 4, 120 keV $^4$He than for A = 3, 160 keV $^3$He. The value of the electron temperature where $W_{crit} = E_{beam}$ for 120 keV $^4$He is only $T_e = 3.3$ keV, which is already available in an ohmically heated plasma. It may therefore be possible to achieve a higher ratio of $T_i/T_e$ than 3 in the Hot-Ion-Hot-Plasma mode of operation. If the target plasma is deuterium, with or without 80 keV deuterium injection from octant 8, then high ion temperatures should be accessible, and all neutron and charge exchange diagnostics can be used as discussed. If we take $T_i/T_e$ of 3, and $E_{dh}$ the average injection energy of a D or H beam, the maximum ion temperature becomes $(120 + E_{dh})/(2.5 + 2\alpha)$. For example, taking $E_{dh} = 60$ keV and $\alpha = 1$ gives $T_i = 40$ keV.

The main advantage of 80 keV H injection is the high energy per nucleon of the full energy component, 80 keV per AMU. This is important from three points of view. First, the injected velocity can exceed the plasma Alfvén velocity, depending on parameters, so that instability studies would be possible. Ion velocities have been achieved in JET in excess of the Alfven velocity by RF

heating, but with high anisotropy (most recent reference [15]. Hydrogen injection allows a more isotropic distribution. However, recent experiments in DIID have not shown any instabilities from H injection into D plasmas. Second, the high energy per nucleon improves the accuracy of charge exchange recombination spectroscopy measurements. Third, since the critical energy is very low for A = 1, the beams become efficient electron heaters, which may be interesting for studies of large electron sawteeth, electron transport, etc.

The penetration, species mix, power fractions, etc. of 70-80 keV H beams are identical to those of 140-160 keV D beams with the same velocity. Since the neutralization efficiency is already falling rapidly at 70-80 keV for H, there is little point in considering higher energy H injection.

We now consider injecting $^3$He at 80 keV. $^3$He at 80 keV has the same velocity as $^4$He at 107 keV. The fusion rate of D-$^3$He is reduced compared to that of 160 keV $^3$He. Also, because of the lower velocity, a high ion temperatures would mean that the ions are being injected into the thermal distribution. For 80 keV $^3$He injected into deuterium, the cutoff of 1.5 $V_{thermal}$ for slowing down integration corresponds to a deuterium temperature of 23.7 keV. The maximum ion temperature from 80 keV $^3$He, for $T_i = 3T_e$, is $(80+E_{dh})/2.5+2\alpha)$. For $E_{dh} = 0$ and $\alpha = 1$. we obtain 17.7 keV.

There are two cases to consider to estimate the D-$^3$He fusion rate, one in which the D-$^3$He plasma is entirely thermal, with $T_i \approx 23$ keV, the other in which the beam-plasma rate is dominant, with a reasonable lower limit of 1.5 $V_{th}$, for example with $T_i = 10$ keV.

For a $T_i$ =23 keV thermal plasma, Fig. 2 shows that $\overline{\sigma v} = 6.8\times10^{-24} m^3 sec^{-1}$, an order of magnitude below that at $T_i = 50$ keV. Fusion power rates would then be much less than 100 kW.

For an 80 keV $^3$He ion slowing down in a $T_e = T_i = 10$ keV plasma, $\overline{\sigma v} = 1.78\times10^{-24} m^3 sec^{-1}$, and Q = 0.00047, which is nearly an order of magnitude below the Q for 160 keV $^3$He. The gamma ray production would not be detectable. As is seen in Fig. 12, where the reaction rate is plotted versus energy during slowing down by the SNAP code, the reaction rate is much lower with 80 keV than with 160 keV injection.

For combined NBI/RF heating, there are many choices from combinations of beam and or plasma H,D,$^3$He, $^4$He. Specific choices and possibilities obviously depend on e/m ratios of the species and their concentrations. Using only H and/or He, neutron-free discharges may be obtained, an important advantage for reducing machine activation, but not for fusion product measurements.

### 3.11 Helium Metastables

The formation of helium metastables could pose serious problems for the operation of helium beams. Metastable can be generated by direct electron capture by fast ions from neutrals; by neutral-neutral collisions, and by combinations of processes. The cross-section for metastable formation by electron capture is about 5%-10% of the cross-section for capture into the ground state.

Takeuchi reported at the EPS conference [16] that he had injected a 200 keV $^4$He beam (equivalent to 150 keV $^3$He) into JT-60 as a diagnostic beam, and that the beam contained 30% metastable ($2s^3S$) atoms which are ionized in the peripheral regions of the plasma. The beam was produced by charge exchange in a thick gas target.

The danger from metastables ionized in the JET plasma edge is that a high heat load could be placed on limiters. If even 1% of the beam is ionized by an ICRH antenna so that it drifts directly into a protection tile, it could destroy the tile. Also, large metastable fractions would reduce the heating power at the plasma axis.

There are several possibilities for dealing with this problem. It may be possible to optimize the JET neutralizer to minimize the metastable fraction in the beam. Experiments are being carried out in the JET testbed. Also, several MW of helium beams were injected into a DIIID divertor plasma, and an H-mode was obtained with no obvious deleterious effects. Therefore, it may be most desirable to inject helium beams into inner wall limiter plasmas or diverted plasmas. For plasmas on the outer belt limiter, the plasma should be kept a safe distance from the ICRF antenna, and short-pulse, low-power beams used for initial tests.

## 4. DETAILS OF EXPERIMENTS

### 4.1 Experiment on: "Standard Operation with $^3$He NBI"

Up to now, the aspects of $^3$He operation have been discussed. If technically possible, $^3$He injection at 160 keV has many advantages, such as good penetration, high $T_i$, low neutron production, etc. Thus, $^3$He injection can be proposed for standard operation in JET as a heating method, and not just for specific experiments. We propose here detailed experiments aimed at specific questions. The plasma is probably a double-null with 4-5 MA or a limiter at 5-7 MA, 2.8 - 3.45 T, and central electron densities of 2-4 x $10^{19}$ $m^{-3}$, with deuterium gas fill.

### 4.2 Experiment on: "Fusion Product and Charge-Exchange Measurements of Ion Velocity Distributions with 160 keV $^3$He NBI"

i) Look for thermal ion and beam velocity distributions and distortions.

ii) Compare ion temperatures deduced by neutron and by charge exchange measurements.

iii) Study the above as a function of plasma density and ion temperature.

### 4.3 Experiment on: "Hot-Ion-Hot-Plasma Experiments at Reactor Temperatures with 160 keV $^3$He NBI"

i) Try to produce ion temperatures in the range of 25 to 50 keV, and study distribution functions

ii) Study production and effects of 100's of kW of isotropic, fast proton production

iii) Study triton production and both beam-plasma and thermal triton burnup and particle confinement time

iv) Try for high-beta at high temperature and pressure, and improve $n\tau T$.

4.4 Experiment on: "Synergistic Effects of Combined 160 keV $^3$He NBI and Minority ICRF Heating"

i) Measure D-$^3$He gamma production to look for synergistic effects.

ii) Compare experiment to code predictions.

iii) Study degree to which anisotropy of fast ion ICRH distribution is affected by injection.

4.5 Experiment on: "Simulation of a-particle Thermalization and Particle Diffusion with 160 keV $^3$He NBI"

i) Study the slowing down distribution function of 160 keV $^3$He.

ii) Study particle diffusion during and after thermalization to simulate reactor a-particle diffusion.

iii) Characterize the minority fraction for use with RF $^3$He heating experiments.

4.6 Experiment on: Effects of Velocity Distributions on Sawteeth, Fishbones, and Alfven Instabilities with 160 keV $^3$He Injection

This experiment involves more a synthesis of results from previously described experiments than a separate experiment.

Sawteeth: IThere is a possibility of studying $T_i$ sawteeth at high temperatures, as discussed in [17].

Fishbones and Alfvén Instabilities: With $^3$He injection with or without RF heating, a wider distribution of velocity distributions is possible. A wider range of isotropic vs perpendicular distributions is avilable for study. The possible intense generation of high energy protons offers new possibilites.

## 4.7 Experiment on: "High Ion Temperature Plasmas with Reduced or Zero Fusion Neutron Emission using H, $^3$He and $^4$He NBI

This experiment can be described as a repeat of the 6 experiments 4.1-4.6, except: octant 4 is run with 120 keV $^4$He or 160 keV $^3$He; octant 8 is run with 80 keV H or 80 keV $^3$He or 80 keV $^4$He. The plasma is run with various fractions of H, $^3$He, $^4$He, and/or some deuterium if some neutron emission is allowed and desired for fusion product diagnostic measurements.

# 5. CONCLUSIONS

The injection of 160 keV $^3$He into JET plasmas allows several interesting experiments, including studies of: fast ion and thermal distributions by means of fusion product and charge exchange diagnostics with separated beam and plasma components; ion temperatures in the 25-50 keV range; synergistic effects of combined NBI/RF; simulation of $\alpha$-particle thermalization and diffusion; sawteeth and instability phonomena; low neutron emission.

Fokker-Planck calculations have been made in support of these experiments. The results at high ion temperatures show the effects of electron and ion energy diffusion of the beam, and profile effects. With $^3$He injection only, D-$^3$He Q values over in the range 0.2% - 2.0% may be obtained. With 10 MW of $^3$He injection and either 10 MW of 80 keV D or 10-20 MW of RF heating, several hundred KW of D-$^3$He power and ion temperatures of 25-50 keV may be produced. New regimes of hot ion distribution functions, triton burnup and combined heating can be investigated.

The high energy per nucleon, the monoenergetic nature, and the double charge-exchange properties of 160 keV $^3$He open new diagnostic possibilities: for fusion product studies by separation into neutron emission from thermal plasma only and gammas from beam-plasma reactions; for charge exchange (CX) studies by CX spectroscopy and active and passive particle CX measurements.

In addition to heating, the beams provide a precise source of particles, and offer the possibility of reduced neutron generation and high performance plasmas. An outstanding problem is the formation of the metastables which would be trapped at the plasma edge.

The detailed experiments proposed offer the possibilities of extending JET's operating parameters and of increasing our understanding of high ion temperature plasmas.

**REFERENCES**


[1] L G Eriksson, T Hellsten et al, Nucl. Fusion 29 (1989) 87.

[2] The JET Team, P R Thomas et al., IAEA-CN-50/A-4-4 (1988).

[3] D A Boyd et. al. Nucl. Fusion 29 (1989) 593.

[4] E Thompson "Injection of Beams of Energetic Helium into JET, NBH Division, Memo ET M1-S6, 1988.

[5] P van Belle and G Sadler, Analysis Code for JET Neutron Group, Private Communication.

[6] L Spitzer, "Physics of Fully Ionized Gases".

[7] T Stix, Plasma Physics 14 (1972) 367.

[8] J G Cordey, W G F Core, Phys. Fluids 17 (1974).

[9] F B Marcus, W Core, "Improved Analytic Solution of the Fokker-Planck Equation for High Ion Temperature, Beam-Heated JET Plasmas," in preparation as JET Report.

[10] F B Marcus et al, "JET Neutron Emission Profiles and Fast Ion Redistribution from Sawteeth". EPS conference, Amsterdam 1990.

[11] L Eriksson and T Hellsten, "Self-consistent calculations of ICRH power deposition and velocity distribution". JET preprint JET-P(89)65, submitted to NUCLEAR FUSION.

[12] G Sadler et al., "Investigations of fast particle behaviour in JET using nuclear techniques". Alpha Particle Workshop, Kiev, 1989, JET Report P(89)77.

[13] M von Hellerman, JET internal memo, 18 Oct. 1989.

[14] M Petrov, "Alpha Particle Diagnostics Using Neutral Particle Analyzers", JET Seminar, 29 Nov 1989, and "Active Charge Exchange Diagnostic of charged Fusion Products in JET Plasmas, JET seminar, 11 April 1990.

[15] G A Cottrell et al, "Alpha Particle Simulation Experiments in JET," Contributed APS Poster (1989)

[16] H Kubo et al, H Takeuchi, EPS Conference, Amsterdam 1990, p. 1508.

[17] F B Marcus, "Fishbones, Sawteeth,...", Neutron Group Seminar, JET Nov. 1989

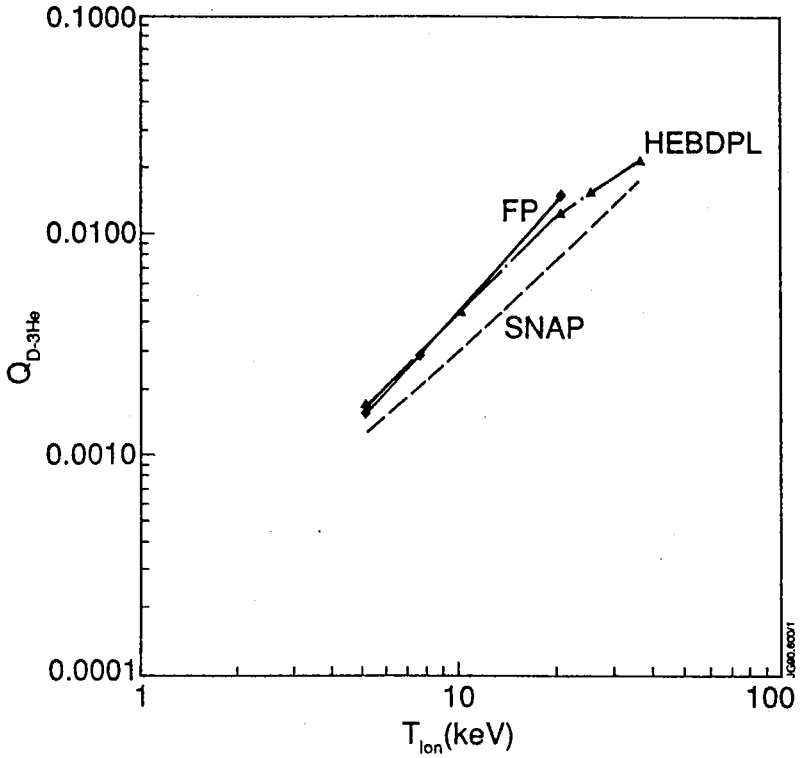


Fig. 1 Beam-plasma $Q_{D-3He}$ versus ion temperature $T_{ion}$(keV) with 160 keV $^3$He neutral beam injection into a $Z_{eff}$=1 deuterium plasma with electron density $N_e=3\times10^{19}$ $m^{-3}$, from the slowing down model in SNAP, the Fokker-Planck code FP, and the improved Fokker-Planck code HEBDPL.

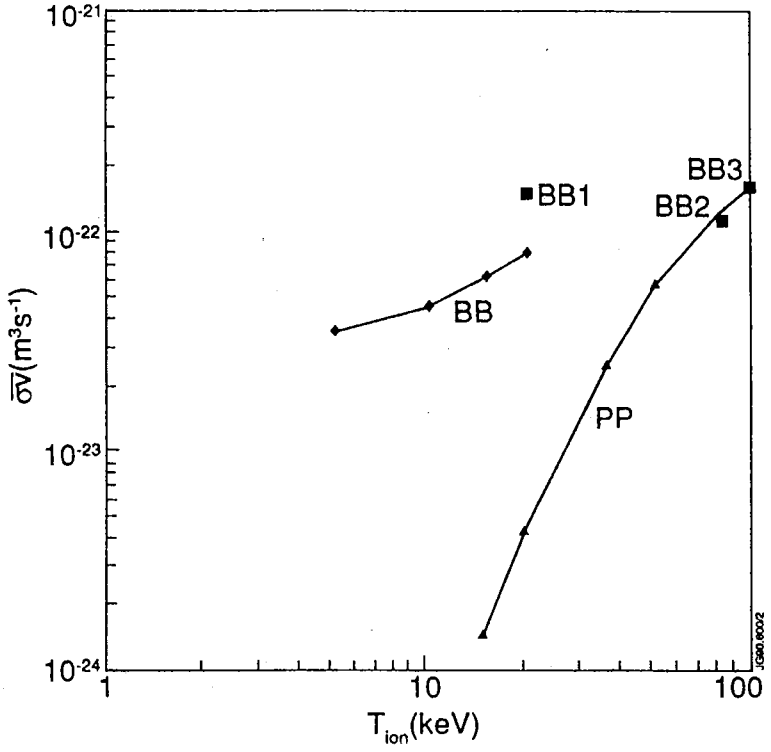


Fig. 2 Beam-beam and plasma-plasma (thermal) reaction rates $\overline{\overline{\sigma v}}$ ($m^{3-1}s^{-1}$) versus plasma ion temperature $T_i$ (keV), with $T_e=T_i$, for deuterium and $^3$He interacting. The reactions are:
PP: plasma-plasma (thermal), D-$^3$He
BB: beam-beam, slowing down distributions of 80 keV D, 160 keV $^3$He
BB1: beam-beam, slowing down distributions of 140 keV D, 160 keV $^3$He
BB2: beam-beam, isotropic, monoenergetic beams of 80 keV D, 160 keV $^3$He
BB3: beam-beam, isotropic, monoenergetic beams of 140 keV D, 160 keV $^3$He

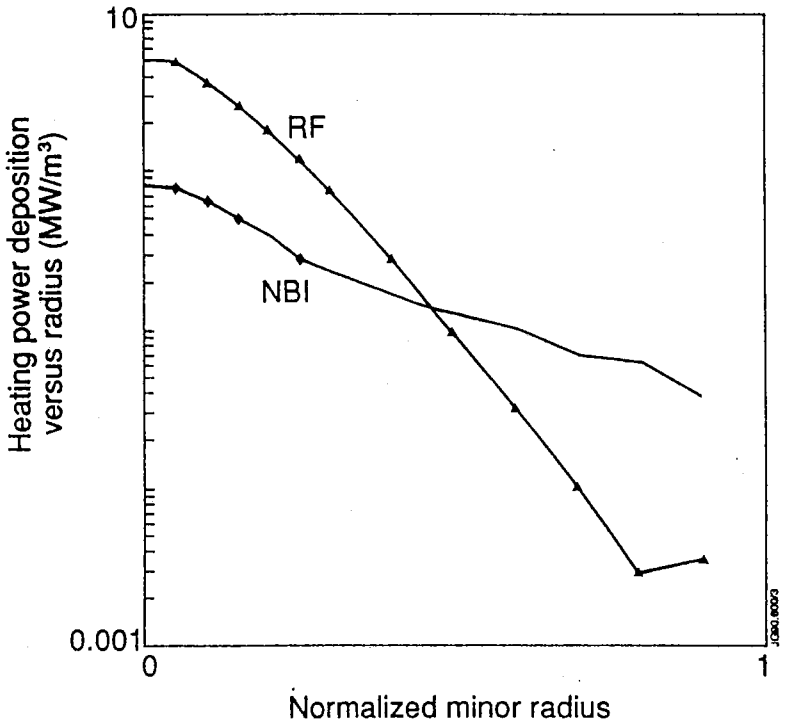


Fig. 3 Heating power deposition versus radius of 20 MW of Ion Cyclotron RF heating and of 10 MW of $^3$He NBI heating. Result of simulation calculations with the PION code. The assumed plasma conditions are: $N_e=4x10^{19}m^{-3}(1-x^2)^{0.55}$, $T_{ion}=25\ keV(1-x^2)^2$, $T_e=T_{ion}/3$, $N_{3He}=0.20xN_{deut}$, NBI of 160 keV $^3$He, dipole RF heating resonant with the $^3$He fundamental

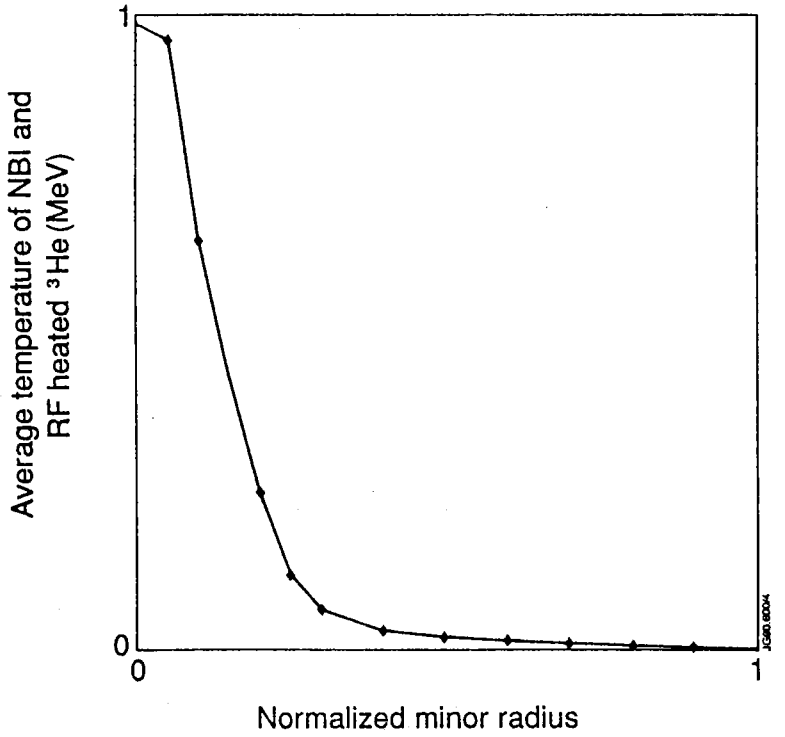


Fig. 4 $^3$He average temperature versus radius with 20 MW of Ion Cyclotron RF heating and of 10 MW of $^3$He NBI heating. Result of simulation calculations with the PION code. The assumed plasma conditions are: $N_e=4x10^{19}m^{-3}(1-x^2)^{0.55}$, $T_{ion}=25\ keV(1-x^2)^2$, $T_e=T_{ion}/3$, $N_{3He}=0.20xN_{deut}$, NBI of 160 keV $^3$He, dipole RF heating resonant with the $^3$He fundamental

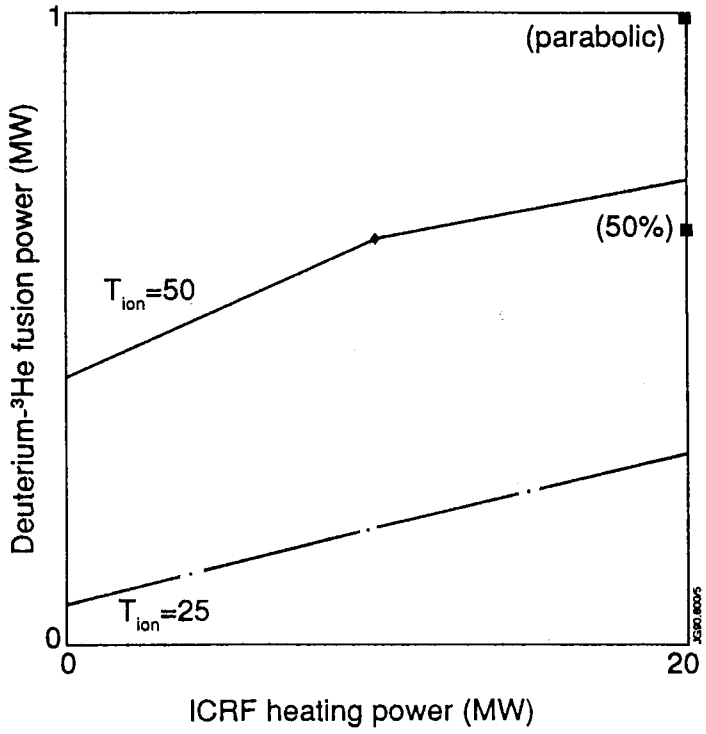


Fig. 5 D-$^3$He fusion power (MW) at 18.35 MeV per fusion versus RF heating power (MW). Result of simulation calculations with the PION code. The assumed plasma conditions are: $N_e=4x10^{19}m^{-3}(1-x^2)^{0.55}$, $T_{ion}=T_{io}$ keV$(1-x^2)^2$, $T_e=T_{ion}/3$, $N_{^3He}=0.20xN_{deut}$, 10 MW of NBI of 160 keV $^3$He, dipole RF heating resonant with the $^3$He fundamental. The ion temperature implicitly simulates the effects of additional NBI heating with deuterium. The parabolic point represents the effects of a temperature profile of $(1-x^2)$, and the 50% represents the 50% minority $^3$He case

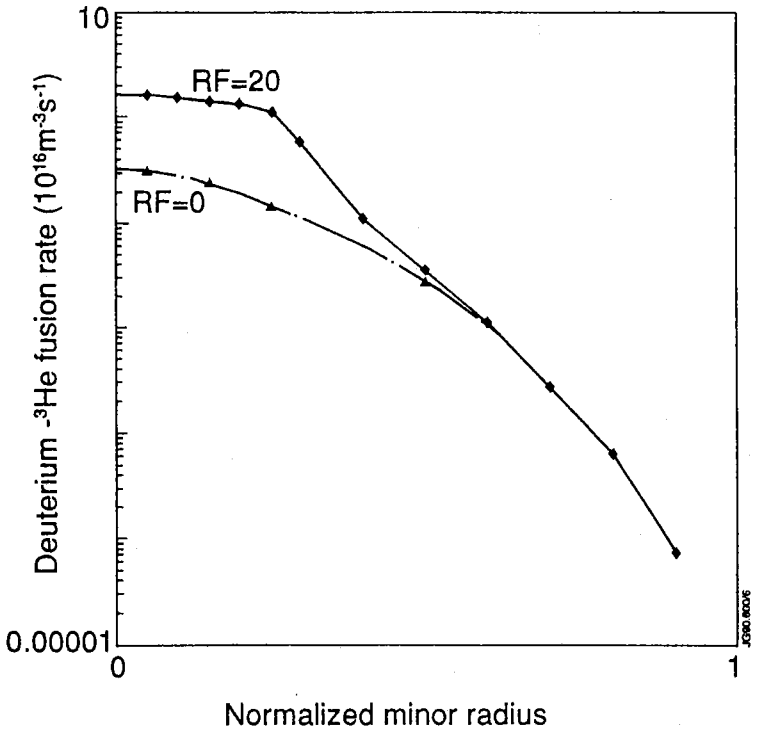


Fig. 6 D-$^3$He fusion rate per unit volume versus radius. Result of simulation calculations with the PION code. The assumed plasma conditions are: $N_e=4x10^{19}m^{-3}(1-x^2)^{0.55}$, $T_{ion}=25$ keV$(1-x^2)^2$, $T_e=T_{ion}/3$, $N_{^3He}=0.20xN_{deut}$, NBI of 160 keV $^3$He, dipole RF heating resonant with the $^3$He fundamental, comparing 0 MW and 20 MW of RF heating

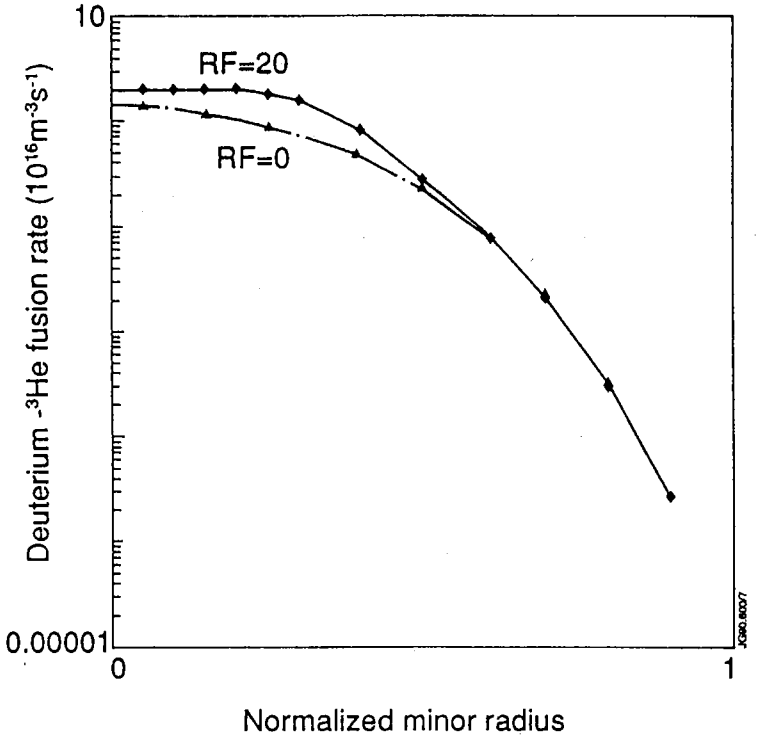


Fig. 7 D-$^3$He fusion rate per unit volume versus radius. Result of simulation calculations with the PION code. The assumed plasma conditions are: $N_e=4x10^{19}m^{-3}(1-x^2)^{0.55}$, $T_{ion}=50$ keV$(1-x^2)^2$, $T_e=T_{ion}/3$, $N_{3He}=0.20xN_{deut}$, NBI of 160 keV $^3$He, dipole RF heating resonant with the $^3$He fundamental, comparing 0 MW and 20 MW of RF heating

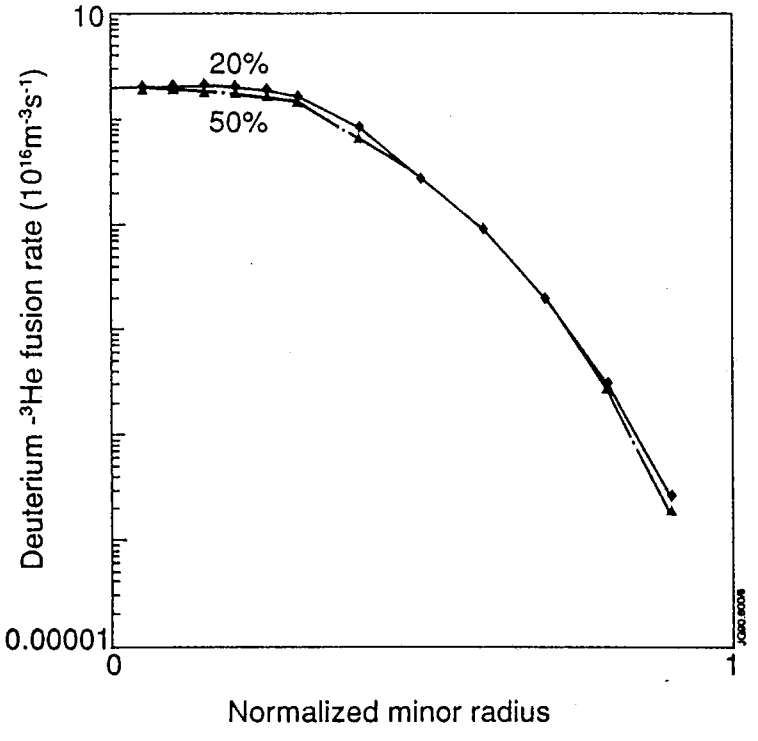


Fig. 8 D-$^3$He fusion rate per unit volume versus radius. Result of simulation calculations with the PION code. The assumed plasma conditions are: $N_e=4x10^{19}m^{-3}(1-x^2)^{0.55}$, $T_{ion}=50$ keV$(1-x^2)^2$, $T_e=T_{ion}/3$, $N_{3He}=0.20$ or $0.50xN_{deut}$, NBI of 160 keV $^3$He, 20 MW of dipole RF heating resonant with the $^3$He fundamental

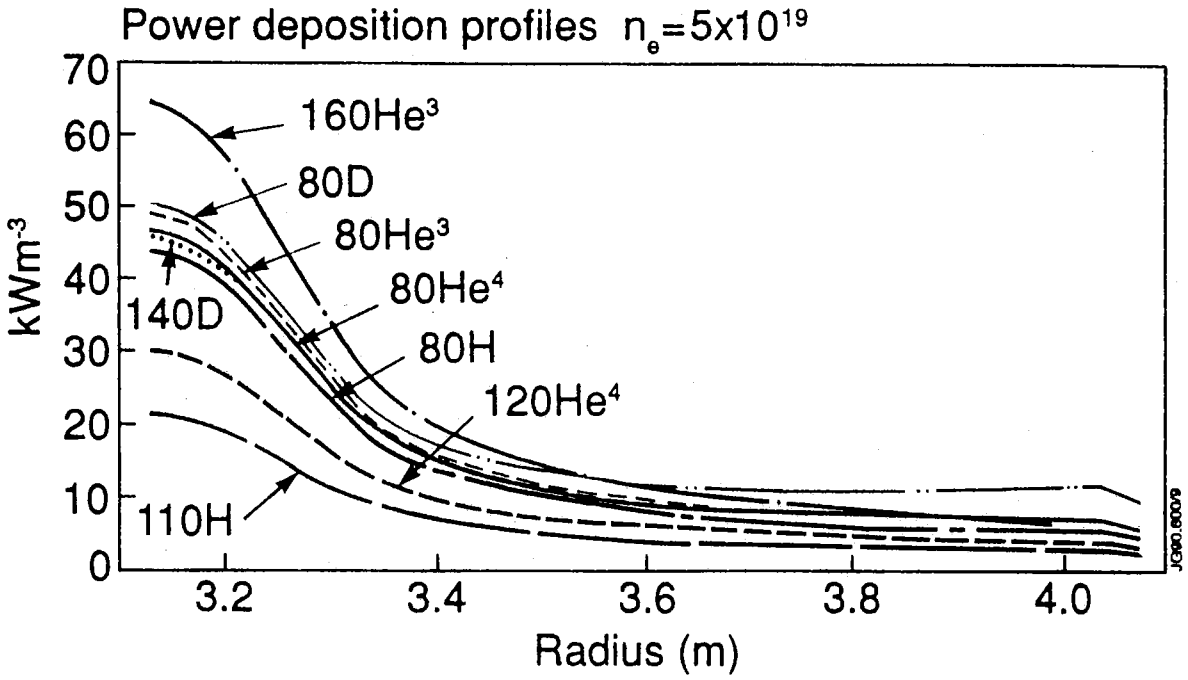


Fig. 9 NBI Power deposition profiles versus plasma major radius for 1 PINI into a D plasma with Zeff=1, Te(0)=8keV, flat electron density profile, $N_e(0)=5\times10^{19}\ m^{-3}$, for different beam extraction voltages and beam gases

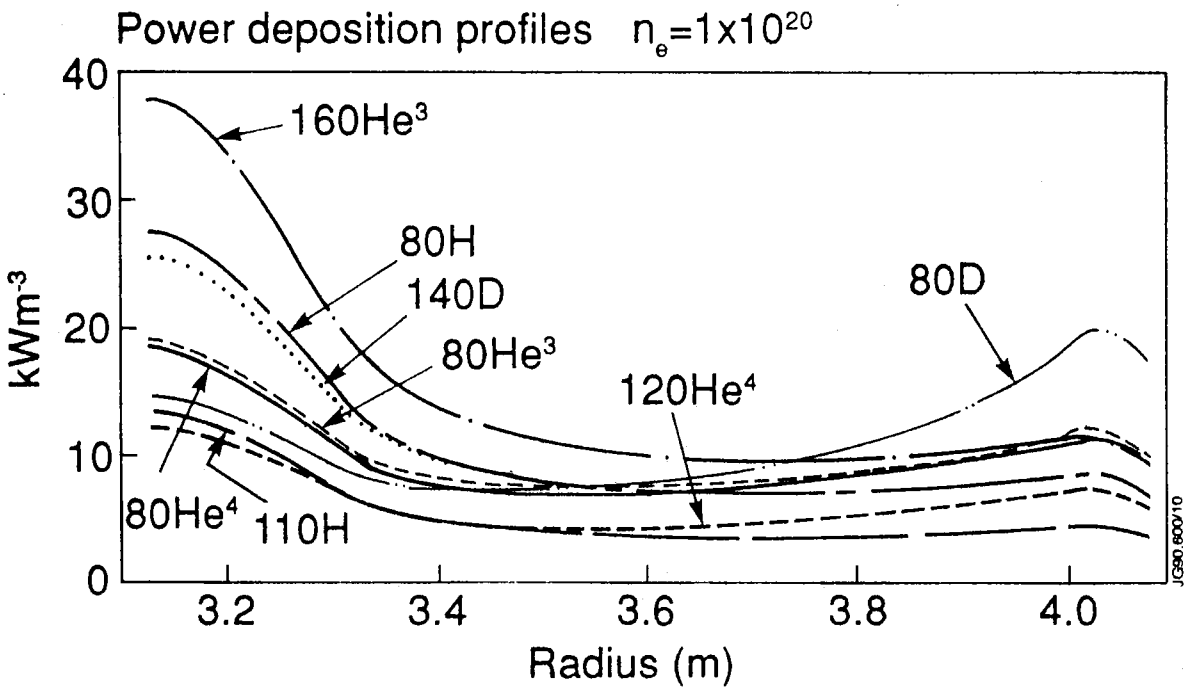


Fig. 10 NBI Power deposition profiles versus plasma major radius for 1 PINI into a D plasma with Zeff=1, Te(0)=8keV, flat electron density profile, $N_e(0)=1\times10^{20}\ m^{-3}$, for different beam extraction voltages and beam gases

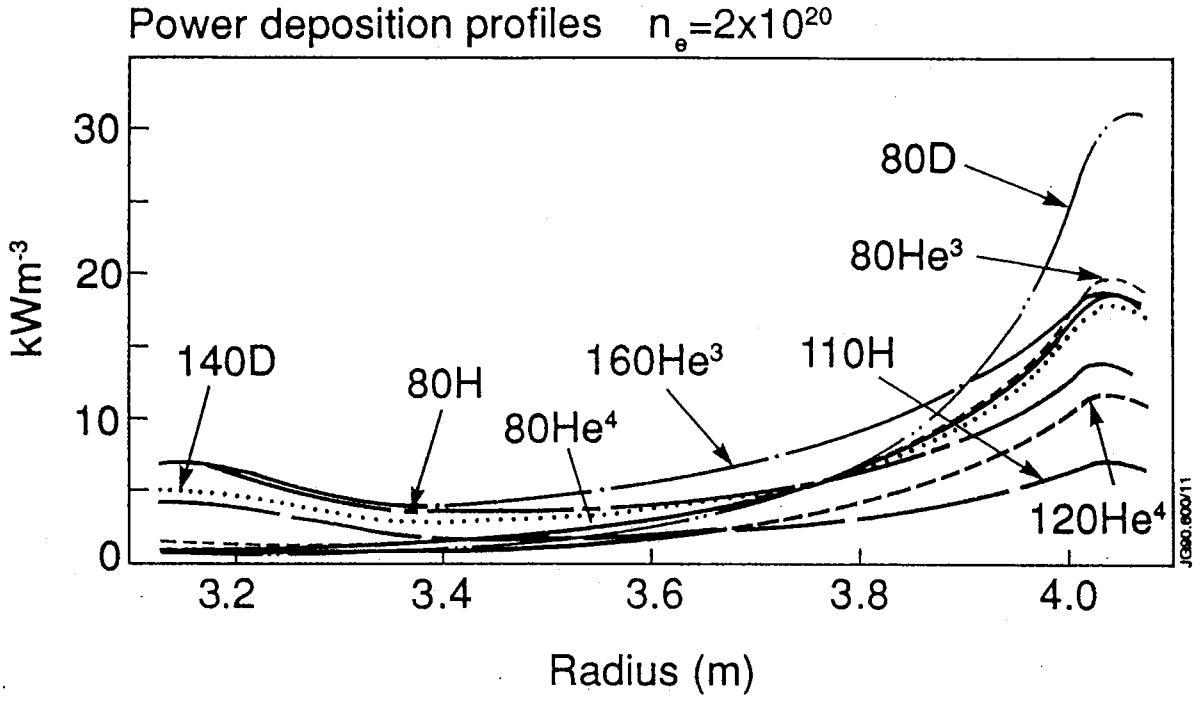


Fig. 11 NBI Power deposition profiles versus plasma major radius for 1 PINI into a D plasma with $Z_{eff}=1$, $T_e(0)=8keV$, flat electron density profile, $N_e(0)=2x10^{20}m^{-3}$, for different beam extraction voltages and beam gases

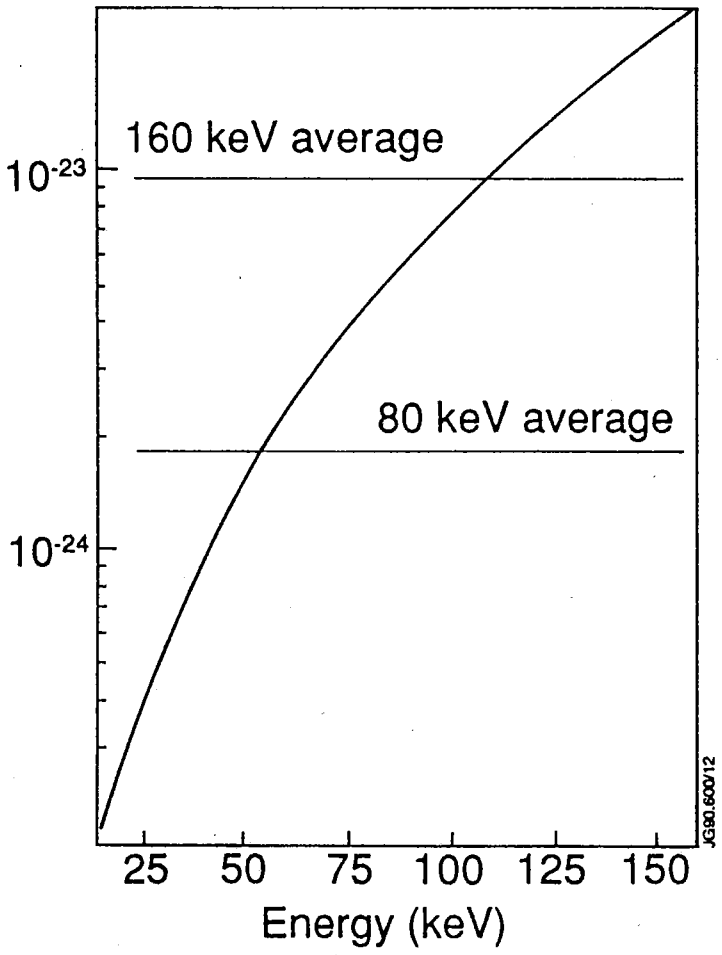


Fig. 12 D-$^3$He reaction rate ($m^3s^{-1}$) versus $^3$He energy during slowing down in a D plasma, with averages shown for initial energies of 80 keV and 160 keV $^3$He. The D plasma has $Z_{eff}=1$, $T_e=T_i=10keV$ and $N_e=3x10^{19}m^{-3}$